Steric Effects in the Chemisorption of Vibrationally Excited Methane on Ni(100)

Bruce L. Yoder, *et al.*

Science **329**, 553 (2010);
DOI: 10.1126/science.1191751

presence of {110} reactive facets, which disappear as the nanoparticles grow. The presence of DCE or similar chlorine-containing compounds yields small nanoparticles of ~3 nm in diameter, exposing the highly reactive {110} facets so as to trigger an oriented-attachment process. Both the oriented attachment and the strong crystalline correlation between the nanosheets in stacked aggregates are most likely driven by the formation of a highly ordered oleic acid bilayer between the PbS nanosheets. The absence of ligands in the in-plane direction of the ultrathin sheets yields a prominent photoconductivity response in the pristine dried nanomaterial.

References and Notes

1. R. L. Penn, J. F. Banfield, *Science* **281**, 969 (1998).
2. J. F. Banfield, S. A. Welch, H. Zhang, T. T. Ebert, R. L. Penn, *Science* **289**, 751 (2000).
3. J. Polleux, N. Pinna, M. Antonietti, M. Niederberger, *Adv. Mater.* **16**, 436 (2004).
4. Y. W. Jun, J. S. Choi, J. Cheon, *Angew. Chem. Int. Ed.* **21**, 3414 (2006).
5. A. J. Houtepen *et al.*, *J. Am. Chem. Soc.* **128**, 6792 (2006).
6. E. Lifshitz *et al.*, *Nano Lett.* **3**, 857 (2003).
7. T. L. Mokari, M. J. Zhang, P. D. Yang, *J. Am. Chem. Soc.* **129**, 9864 (2007).
8. J. S. Steckel, B. K. H. Yen, D. C. Oertel, M. G. Bawendi, *J. Am. Chem. Soc.* **128**, 13032 (2006).
9. K. T. Yong, Y. Sahoo, M. T. Swihart, P. N. Prasad, *J. Phys. Chem. C* **111**, 2447 (2007).
10. B. H. Juárez *et al.*, *J. Am. Chem. Soc.* **130**, 15282 (2008).
11. J. S. Son *et al.*, *Angew. Chem. Int. Ed.* **48**, 6861 (2009).
12. Z. Y. Tang, Z. Zhang, Y. Wang, S. C. Glotzer, N. A. Kotov, *Science* **314**, 274 (2006).
13. H. G. Yang, H. C. Zeng, *Angew. Chem. Int. Ed.* **43**, 5930 (2004).
14. Z. Huo *et al.*, *Nano Lett.* **9**, 1260 (2009).
15. M. Nagel, G. S. Hickey, A. Frömsdorf, A. Kornowski, H. Weller, *Z. Phys. Chem.* **221**, 427 (2007).
16. K. S. Cho, D. V. Talapin, W. Gaschler, C. B. Murray, *J. Am. Chem. Soc.* **127**, 7140 (2005).
17. J. J. Urban, D. V. Talapin, E. V. Shevchenko, C. B. Murray, *J. Am. Chem. Soc.* **128**, 3248 (2006).
18. T. Duan, W. Lou, X. Wang, Q. Xue, *Colloids Surf. A Physicochem. Eng. Asp.* **310**, 86 (2007).
19. E. Capek, K. E. Schwarzhans, *Monatsh. Chem.* **118**, 419 (1987).
20. F. Kaneko *et al.*, *J. Phys. Chem. B* **101**, 1803 (1997).
21. S. R. Craig *et al.*, *J. Cryst. Growth* **128**, 1263 (1993).
22. S. Abrahamsson, I. Ryderstedt-Nahringbauer, *Acta Crystallogr.* **15**, 1261 (1962).
23. M. S. Nikolic *et al.*, *Angew. Chem. Int. Ed.* **48**, 2752 (2009).
24. D. V. Talapin, C. B. Murray, *Science* **310**, 86 (2005).
25. J. M. Luther *et al.*, *ACS Nano* **2**, 271 (2008).
26. M. V. Kovalenko, M. Scheele, D. V. Talapin, *Science* **324**, 1417 (2009).
27. K. Szendrei *et al.*, *Adv. Mater.* **21**, 683 (2009).
28. T. S. Mentzel *et al.*, *Phys. Rev. B* **77**, 075316 (2008).
29. G. Konstantanos *et al.*, *Nature* **442**, 180 (2005).

30. B.H.J. thanks the European Commission for grant ERG FP7-PEOPLE-ERG-2008 and the Spanish Ministry of Science and Innovation for grant RYC-2007-01709.

Supporting Online Material

www.sciencemag.org/cgi/content/full/329/5991/550/DC1
Materials and Methods
Figs. S1 to S11
References

8 February 2010; accepted 30 June 2010
10.1126/science.1188035

Steric Effects in the Chemisorption of Vibrationally Excited Methane on Ni(100)

Bruce L. Yoder, Régis Bisson, Rainer D. Beck*

Newly available, powerful infrared laser sources enable the preparation of intense molecular beams of quantum-state prepared and aligned molecules for gas/surface reaction dynamics experiments. We present a stereodynamics study of the chemisorption of vibrationally excited methane on the (100) surface of nickel. Using linearly polarized infrared excitation of the C-H stretch modes of two methane isotopologues [$CH_4(\nu_3)$ and $CD_3H(\nu_1)$], we aligned methane's angular momentum and vibrational transition dipole moment in the laboratory frame. An increase in methane reactivity of as much as 60% is observed when the laser polarization is parallel rather than normal to the surface. The dependence of the alignment effect on the rotational branch used for excitation indicates that alignment of the vibrational transition dipole moment of methane is responsible for the steric effect. Potential explanations for the steric effect in terms of an alignment-dependent reaction barrier height or electronically nonadiabatic effects are discussed.

The need to understand the dynamics of gas/surface reactions is driven by the critical role that these reactions play in many industrial processes, such as heterogeneous catalysis for molecular synthesis and chemical vapor deposition of thin films. Highly detailed state-resolved measurements are required to reveal the underlying microscopic dynamics and reaction mechanisms. Quantum-state–resolved data also enable stringent tests of theoretical models of gas/surface reactivity. The choice of methane chemisorption on a Ni surface as a model system is pragmatic, because C-H bond activation of this system is the rate-limiting step in steam reforming of CH_4 to produce industrial hydrogen and syngas, the starting material for the synthesis of many commercial compounds.

In the late 1970s, the use of molecular beams for reactivity measurements on single-crystal surfaces enabled the preparation of reactant molecules with well-defined translational energy and incident angle. Molecular beam studies clearly demonstrated that the translational energy of the incident CH_4 activates its chemisorption (*1*). Laser excitation of methane isotopologues to specific rovibrational quantum states (*2*–*4*) further refined the measurements, providing unequivocal evidence that the chemisorption is also activated by vibrational excitation of the incident methane molecule in a mode- (*5*) and bond-specific (*6*) manner that statistical models (*7*) fail to capture.

In the experiments described here, we move a step beyond quantum-state resolution, by exerting steric control over this gas/surface reaction. Excitation by linearly polarized infrared radiation prepares CH_4 in a single rovibrationally excited state with aligned angular momentum $\vec{J}$ and vibrational transition dipole moment $\vec{\mu}_{if}$ in the laboratory frame (*8*). The resulting aligned, state-prepared reactants are used to detect and

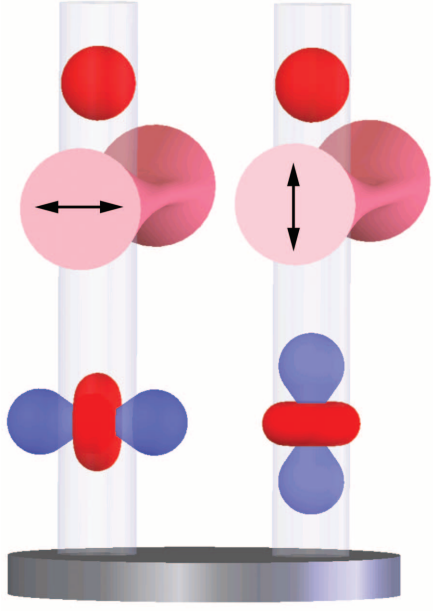

Fig. 1. Schematic of the state-prepared and laser-aligned molecular beam deposition experiment. A molecular beam of CH_4 with initially isotropic spatial distribution of angular momentum $\vec{J}$ (indicated by the red spheres at top) impinges on a Ni(100) surface at normal incidence. Before surface impact, the molecules traverse a continuous, linearly polarized laser beam focused in the direction of the molecular beam. Incident CH_4 is prepared in a specific rovibrationally excited state by rapid adiabatic passage (*16*) through the resonant laser beam. The resulting probability distributions for $\vec{J}$ (red) and vibrational transition dipole moment $\vec{\mu}_{if}$ (blue) are depicted for the case of R(0) excitation and two orthogonal polarization directions indicated by the double-headed arrows.

Laboratoire de Chimie Physique Moléculaire, Ecole Polytechnique Fédérale de Lausanne, Lausanne, Switzerland.

*To whom correspondence should be addressed. E-mail: rainer.beck@epfl.ch

quantify steric effects in the reaction of vibrationally excited methane isotopologues with a Ni(100) surface. Here, alignment refers to an anisotropic spatial distribution of $\vec{J}$ and $\vec{\mu}_{if}$ vectors, which is either preferentially parallel or perpendicular to a laboratory fixed axis such as the electric field vector $\vec{E}$ of the excitation laser. In contrast, orientation describes a preference in vectorial direction of $\vec{J}$ and $\vec{\mu}_{if}$ (i.e., parallel or antiparallel) relative to $\vec{E}$.

Polanyi highlighted the opportunity to study stereodynamics in surface reactions, given that a single-crystal surface represents a perfectly oriented reaction partner (*9*). What is needed to completely define the collision geometry in a gas/surface reaction is a method to orient or align incident molecules relative to the surface plane. Several techniques have been used to study alignment and orientation effects in gas/surface reactions, such as hexapole state-selection followed by reactant orientation in a static electric field (*10*, *11*), reactant alignment by resonance-enhanced multiphoton ionization (REMPI) by linearly polarized light (*12*), and collisional rotational alignment in supersonic jet expansions (*13*). Another method to obtain information about gas/surface stereodynamics is linearly polarized REMPI of molecules desorbing from a surface, coupled with analysis using the principle of detailed balance (*14*, *15*). Unfortunately, none of these techniques is applicable to CH_4.

In contrast to previous stereodynamical studies of gas/surface reactions, our experiments align molecules without permanent dipole moments and probe specifically the alignment-dependent reactivity of vibrationally excited neutral reactant molecules. We explore whether the reactivity of vibrationally excited CH_4 depends on the alignment of $\vec{J}$ and/or $\vec{\mu}_{if}$ relative to the surface plane, with the aim of elucidating the mechanism of the vibrationally mode-specific reactivity (*5*), which is not fully understood.

We performed the experiments in a surface science–molecular beam apparatus (*4*, *16*). First, we exposed the Ni(100) surface in two different locations to an identical dose of vibrationally excited $CH_4(\nu_3)$, prepared with one quantum of the antisymmetric C-H stretch vibration ν_3, via the R(0) transition at 3028.75 cm^{-1} but with different laser polarization directions (Fig. 1). Then, quantum-state–resolved reaction probabilities were measured using Auger electron spectroscopy detection of surface-bound C. Comparison of the detected amount of surface carbon (C) resulting from the two depositions indicated that the CH_4 reactivity is up to 60% higher for ν_3-R(0) excitation (Fig. 2, top) with the laser polarization parallel to the plane of the surface than for perpendicular polarization. The observed alignment effect was quantified by calculating the alignment contrast Δ_p

$$\Delta_p = \frac{S_0^{\parallel} - S_0^{\perp}}{S_0^{\parallel} + S_0^{\perp}} \quad (1)$$

where $S_0^{\parallel}$ and $S_0^{\perp}$ are state-resolved initial reaction probabilities for the excited state of CH_4 prepared with laser polarization parallel and perpendicular to the surface plane, respectively. Based on nine repeated measurements, $\Delta_p = 0.216 \pm 0.016$ for excitation of the ν_3-R(0) transition of CH_4, with error limits of $\pm 2\sigma$ from the standard deviation of replicate measurements.

In order to ascertain whether the observed reactivity difference is due solely to alignment effects of the vibrationally excited CH_4, we performed the corresponding pair of depositions using excitation via the ν_3-P(1) transition, which produces no alignment of the excited molecules (*8*). In agreement with our interpretation, we observed no significant difference between the $CH_4(\nu_3)$ reactivity for parallel and perpendicular laser polarizations ($\Delta_p = 0.016 \pm 0.029$, four measurements) for excitation via the ν_3-P(1) transition (Fig. 2, middle). We verified that the detected C is formed exclusively by chemisorption of ν_3-excited CH_4 by repeating the deposition experiment with the excitation laser slightly detuned from the ν_3 resonance. With the laser off-resonance, no C signal was detectable on the surface where the molecular beam had impinged (Fig. 2, bottom). Corresponding measurements for ν_1-excited trideuteromethane, CD_3H, yielded $\Delta_p = 0.178 \pm 0.028$ for the ν_1-R(0) transition and $\Delta_p = 0.009 \pm 0.015$ for the ν_1-P(1) transition, where ν_1 is the C-H stretch normal mode of CD_3H with a band origin at 2993 cm^{-1}.

In our experimental setup, the homogeneous linewidths of the rovibrational transitions are dominated by transit time broadening to more than 1 MHz. Because the hyperfine splittings for CH_4 and CD_3H are in the range of 50 to 200 kHz, the laser coherently excites all hyperfine levels when the methane molecules pass through the excitation laser beam. After excitation at time $t = 0$, the interaction between methane's nuclear spin and $\vec{J}$ leads to a dephasing of the hyperfine components, which scrambles alignment created at $t = 0$ on a time scale of the inverse of methane's hyperfine splitting. By measuring Δ_p for excitation of the R(0) transition at distances between 1 and 30 mm from the target surface, we extracted a time scale for the $CH_4(\nu_3)$ hyperfine dephasing of ≈15 μs (fig. S2). Hyperfine depolarization was observed to be faster for CD_3H (≈5 μs) than for CH_4, which is in agreement with the larger splitting of CD_3H hyperfine levels (*8*). Extrapolation of the measured hyperfine decay of Δ_p toward $t = 0$ predicts an insignificant reduction for excitation at 1 mm from the surface, compared to a hypothetical preparation directly on the surface.

To explore the origin of the alignment dependence of the $CH_4(\nu_3)$ and $CD_3H(\nu_1)$ surface reactivity, we determined the alignment contrast Δ_p for excitation via R-, Q-, and P-branch transitions (fig. S3) and compared the experimental results to calculated alignment coefficients for angular momentum $A_0^{(2)}$ and vibrational transition dipole moment β_{axis}, using expressions given by Zare and others (*17*–*19*). Inspection of Fig. 3A shows a sign change for $A_0^{(2)}$ when switching from R- to Q-branch excitation, whereas the β_{axis} coefficients remain positive (Fig. 3B). The fact that

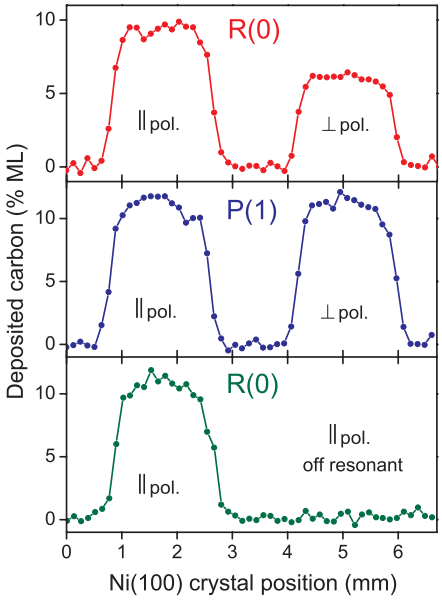

Fig. 2. Auger-detected C signal resulting from exposure of a clean Ni(100) surface to $CH_4(\nu_3)$ with translational energy of 34 kJ/mol, rovibrationally excited 1 mm upstream of the surface, irradiated with laser polarization parallel (II pol.) or perpendicular (⊥ pol.) to the surface plane. (**Top**) $CH_4(\nu_3)$ excited via R(0). (**Middle**) $CH_4(\nu_3)$ excited via P(1). (**Bottom**) $CH_4(\nu_3)$ excited via R(0) (left) and CH_4 irradiated by laser output detuned from resonance (right). Surface temperature is 473 K in all cases.

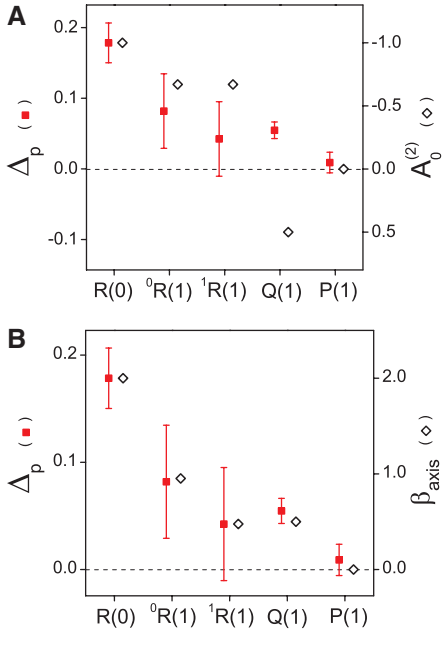

Fig. 3. Comparison of the observed alignment contrast Δ_p for $CD_3H(\nu_1 = 1)$ with (**A**) the angular momentum alignment coefficient $A_0^{(2)}$ and (**B**) the vibrational alignment coefficient β_{axis}. The vertical axes of the graphs are scaled so that their origins and the values associated with R(0) excitation coincide for Δ_p and $A_0^{(2)}$ in (A) and Δ_p and β_{axis} in (B). Error bars are $\pm 2\sigma$ from replicate measurements.

alignment contrasts Δ_p for $CD_3H(\nu_1)$ (Fig. 3) and $CH_4(\nu_3)$ (fig. S10) are positive for both R- and Q-branch transitions and scale with β_{axis} leads us to conclude that the observed reactivity enhancement is due to an alignment of the vibrational transition dipole moment $\vec{\mu}_{if}$ rather than the angular momentum $\vec{J}$, which is similar to the findings of Simpson *et al*. for the reaction of vibrationally excited CH_4 and CD_3H with gas-phase Cl atoms (*8*).

To map out the polarization angle dependence of the alignment effect, we measured the reactivity for $CH_4(\nu_3)$ and $CD_3H(\nu_1)$ for R(0) excitation at several intermediate polarization angles, in addition to 0° (∥ pol) and 90° (⊥ pol). The results (figs. S11 and S12) show a continuous decrease in reactivity from the highest reactivity for parallel polarization to the lowest reactivity for perpendicular polarization for both $CH_4(\nu_3)$ and $CD_3H(\nu_1)$.

In dynamical stereochemistry, the preferred reactant bond alignment reflects the minimum energy path from reactants to products on the multidimensional potential energy surface (PES) via the reaction's transition state. For example, the state-resolved experiments of Hou *et al*. (*14*) imply a much higher reactivity for broadside than for end-on collisions of D_2 with Cu(111) at low collision energy, indicating an alignment-dependent barrier height for this reaction, with a minimum barrier occurring for a D-D bond alignment parallel to the surface. However, for CH_4 dissociation on transition metals, calculations of the transition state structure for the dissociation of CH_4 on Ni(100) (*20*–*22*) predict the dissociating C-H bond to be elongated and oriented toward the surface at nearly 45° from the surface normal and barrier heights ranging from 60 to 90 kJ/mol.

Excitation of the infrared-active C-H stretch fundamentals $CH_4(\nu_3)$ and $CD_3H(\nu_1)$ by linearly polarized light aligns the vibrational transition dipole moment; i.e., the net C-H stretch, preferentially along the laser polarization axis. For $CD_3H(\nu_1)$, where $\vec{\mu}_{if}$ is along the C-H bond axis, the excitation also aligns the C-H bond. Recent state-resolved experiments proved this reaction to be bond-specific by demonstrating that the excited C-H bond dissociates selectively in the chemisorption of $CD_3H(\nu_1)$ on Ni(111) (*6*).

In comparing the polarization direction leading to the highest reactivity of $CD_3H(\nu_1)$ on Ni(100) with the calculated transition state structure (*20*–*22*), one must consider that the laser excitation defines alignment and not orientation of the C-H bond in CD_3H. Excitation with ∥ polarization aligns the excited C-H bond preferentially parallel to the surface plane, whereas ⊥ polarization produces $CD_3H(\nu_1)$ with the C-H bond along the surface normal, but pointing either toward the surface or away from it. Our measurements therefore probe the average reactivity between the two orientations compatible with a given alignment direction. Such averaging could shift the maximum in the angle dependence away from the transition state angle and toward the parallel polarization direction if C-H orientations pointing away from the surface are nearly nonreactive and the variation in reactivity for C-H bond orientations toward the surface is small.

However, the observation of very similar polarization angle dependences for the reactivity of aligned $CD_3H(\nu_1)$ and $CH_4(\nu_3)$ with larger Δ_p values for $CH_4(\nu_3)$ is inconsistent with the idea that the polarization angle dependence reflects the transition state geometry of the reaction. $CH_4(\nu_3)$ has four identical C-H bonds with tetrahedral geometry that share the antisymmetric stretch excitation of the ν_3 normal mode. The reactivity of $CH_4(\nu_3)$ on Ni(100) should show a different polarization angle dependence and smaller Δ_p values than what is observed for $CD_3H(\nu_1)$ if the orientation of the vibrating C-H bond relative to the transition state geometry were to determine the enhancement. In fact, R(0) excitation by linearly polarized light prepares $CH_4(\nu_3)$ in a state with $J = 1$, $l = 1$, and $N = 0$ (*8*), where J, l, and N designate the total, vibrational, and rotational angular momentum, respectively. This state of $CH_4(\nu_3)$ is rotationless ($N = 0$); i.e., it is characterized by a spatially isotropic rotational wave function for which any orientation of the H atoms is equally probable. Classically, CH_4 in this state can be visualized as an ellipsoid vibrating along a principal axis, with the H atoms located on the ellipsoidal surface with unknown orientation (*8*). The direction of the laser polarization controls the alignment of the principal axis of the vibrating ellipsoid without specifying the C-H bond alignment of CH_4. The fact that we observed the highest alignment effect ($\Delta_p = 0.216 \pm 0.016$) for this rotationless state of $CH_4(\nu_3)$ is a strong indication that the observed steric effects are due to the net C-H stretch alignment rather than C-H bond alignment.

The underlying mechanism for the alignment-dependent reactivity of vibrationally excited methane on Ni(100) is not obvious. The higher dissociation probability of methane with the net C-H stretch aligned parallel to the surface could be due to either an alignment dependence of the dissociation probability of the vibrationally excited molecule or to an alignment dependence of the rate of vibrational energy transfer to the surface.

A canonical interpretation explains our results in terms of an alignment-dependent barrier height on a multidimensional reactive PES for the methane/surface system. Dynamical calculations of methane dissociation on a realistic PES with up to 15 degrees of freedom may be needed to understand which degrees of freedom play a decisive role in the observed steric effects. Such a high-dimensional PES [based on the Born-Oppenheimer (BO) approximation] and corresponding dynamics simulations are being developed (*23*) to arrive at a predictive understanding of this important reaction. Our state-resolved, alignment-dependent data can guide such calculations.

Alternatively, the alignment dependence could be due to steric effects in vibrational relaxation rate between the vibrationally excited, incident methane and electron-hole (e-h) pair excitations in the Ni surface (*24*). An early model for vibrational energy transfer between a vibrating molecule and a metal surface (*25*) consists of an oscillating dipole interacting with its electric image dipole induced in the conducting surface. A classical calculation (*26*), treating vibrational relaxation as ohmic dissipation of the induced image current, predicts a maximum dissipation rate for dipole alignment perpendicular to the surface plane, which is twice the minimum rate calculated for parallel dipole alignment. The higher predicted dissipation rate for the perpendicular dipole is consistent with the lower reactivity for this alignment direction if vibrational energy transfer to e-h pairs were significant during the approach of a vibrating methane molecule toward the metal surface.

The image dipole model could also explain the mode-specific reactivity previously observed in comparing the isoenergetic symmetric and antisymmetric C-H stretch normal modes ν_3 and ν_1 of CH_4 (*2*, *27*). In contrast to the infrared-active ν_3 mode, the ν_1-normal mode of CH_4 is only Raman-active and carries no vibrational transition dipole moment from the ground state. Therefore, $CH_4(\nu_1)$ cannot induce an image dipole in the metal surface, which excludes this potential pathway for vibrational energy transfer for ν_1. A $CH_4(\nu_1)$ reactivity observed to be up to 10-fold higher (*27*) than for $CH_4(\nu_3)$ (*2*) is consistent with this model. However, there is currently no direct experimental evidence that e-h pair excitation occurs on the subpicosecond time scale of the reactive collisions of vibrationally excited CH_4 with a metal surface. Theoretical modeling beyond the BO approximation, including the participation of electronically nonadiabatic channels (*28*), should be pursued to shed light on the important question of whether e-h pair excitation plays a significant role in CH_4 chemisorption.

Irrespective of the mechanism, observation that the methane reactivity depends on the initial vibrational alignment, prepared far from the surface, implies the absence of significant steering effects under our experimental conditions. In other words, anisotropic molecule/surface interactions are unable to orient or steer the incident molecule into its lowest-energy reaction path on the subpicosecond time scale of the reactive collision in our experiments.

Furthermore, the observation of an alignment-dependent reactivity of methane on Ni(100) constitutes further evidence for a nonstatistical mechanism of methane chemisorption, beyond the previously reported mode specificity (*5*) and bond selectivity (*6*). Our results show that methane's reaction probability is not simply controlled by the available (vibrational) energy but is state-specific and sensitive to C-H stretch alignment. These observations are incompatible with statistical rate theory, which assumes complete randomization of

initial conditions in the collision complex and predicts reaction rates solely on the basis of energetics (*7*).

References and Notes

1. S. T. Ceyer, D. J. Gladstone, M. McGonigal, M. T. Schulberg, in *Investigations of Surfaces and Interfaces: Part A* (Wiley, New York, 1993).
2. L. B. F. Juurlink, P. R. McCabe, R. R. Smith, C. L. DiCologero, A. L. Utz, *Phys. Rev. Lett.* **83**, 868 (1999).
3. J. Higgins, A. Conjusteau, G. Scoles, S. L. Bernasek, *J. Chem. Phys.* **114**, 5277 (2001).
4. M. P. Schmid, P. Maroni, R. D. Beck, T. R. Rizzo, *Rev. Sci. Instrum.* **74**, 4110 (2003).
5. R. D. Beck *et al.*, *Science* **302**, 98 (2003).
6. D. R. Killelea, V. L. Campbell, N. S. Shuman, A. L. Utz, *Science* **319**, 790 (2008).
7. H. L. Abbott, A. Bukoski, I. Harrison, *J. Chem. Phys.* **121**, 3792 (2004).
8. W. R. Simpson, T. P. Rakitzis, S. A. Kandel, A. J. Orr-Ewing, R. N. Zare, *J. Chem. Phys.* **103**, 7313 (1995).
9. J. C. Polanyi, R. J. Williams, *J. Chem. Phys.* **88**, 3363 (1988).
10. E. W. Kuipers, M. G. Tenner, A. W. Kleyn, S. Stolte, *Phys. Rev. Lett.* **62**, 2152 (1989).
11. M. Brandt, T. Greber, N. Bowering, U. Heinzmann, *Phys. Rev. Lett.* **81**, 2376 (1998).
12. J. N. Greeley, J. S. Martin, J. R. Morris, D. C. Jacobs, *J. Chem. Phys.* **102**, 4996 (1995).
13. L. Vattuone *et al.*, *Angew. Chem. Int. Ed.* **43**, 5200 (2004).
14. H. Hou, S. J. Gulding, C. T. Rettner, A. M. Wodtke, D. J. Auerbach, *Science* **277**, 80 (1997).
15. W. A. Diño, H. Kasai, O. Ayao, *Phys. Rev. Lett.* **78**, 286 (1997).
16. Materials and methods are available as supporting material on *Science* Online.
17. C. H. Greene, R. N. Zare, *Phys. Rev. A* **25**, 2031 (1982).
18. R. N. Zare, *Angular Momentum: Understanding Spatial Aspects in Chemistry and Physics* (Wiley, New York, 1988).
19. E. H. Van Kleef, I. Powis, *Mol. Phys.* **96**, 757 (1999).
20. O. Swang, K. Faegri, O. Gropen, U. Wahlgren, P. Siegbahn, *Chem. Phys.* **156**, 379 (1991).
21. Y. A. Zhu, Y. C. Dai, D. Chen, W. K. Yuan, *J. Mol. Catal. Chem.* **264**, 299 (2007).
22. A. K. Tiwari, S. Nave, B. Jackson, *J. Chem. Phys.* **132**, 134702 (2010).
23. S. Nave, B. Jackson, *Phys. Rev. B* **81**, 233408 (2010).
24. A. M. Wodtke, D. Matsiev, D. J. Auerbach, *Prog. Surf. Sci.* **83**, 167 (2008).
25. B. N. J. Persson, M. Persson, *Solid State Commun.* **36**, 175 (1980).
26. B. N. J. Persson, S. Andersson, *Phys. Rev. B* **29**, 4382 (1984).
27. P. Maroni *et al.*, *Phys. Rev. Lett.* **94**, 246104 (2005).
28. N. Shenvi, S. Roy, J. C. Tully, *Science* **326**, 829 (2009).

29. We thank A. C. Luntz for helpful discussions. Financial support was provided by the Swiss National Science Foundation (grant no. 124666) and the École Polytechnique Fédérale de Lausanne.

Supporting Online Material

www.sciencemag.org/cgi/content/full/329/5991/553/DC1
Materials and Methods
Figs. S1 to S12
References

3 May 2010; accepted 2 July 2010
10.1126/science.1191751

Decrease in the CO_2 Uptake Capacity in an Ice-Free Arctic Ocean Basin

Wei-Jun Cai,[1]* Liqi Chen,[2] Baoshan Chen,[1] Zhongyong Gao,[2] Sang H. Lee,[3] Jianfang Chen,[4] Denis Pierrot,[5,6] Kevin Sullivan,[5,6] Yongchen Wang,[1] Xinping Hu,[1] Wei-Jen Huang,[1] Yuanhui Zhang,[2] Suqing Xu,[2] Akihiko Murata,[7] Jacqueline M. Grebmeier,[8] E. Peter Jones,[9] Haisheng Zhang[4]

It has been predicted that the Arctic Ocean will sequester much greater amounts of carbon dioxide (CO_2) from the atmosphere as a result of sea ice melt and increasing primary productivity. However, this prediction was made on the basis of observations from either highly productive ocean margins or ice-covered basins before the recent major ice retreat. We report here a high-resolution survey of sea-surface CO_2 concentration across the Canada Basin, showing a great increase relative to earlier observations. Rapid CO_2 invasion from the atmosphere and low biological CO_2 drawdown are the main causes for the higher CO_2, which also acts as a barrier to further CO_2 invasion. Contrary to the current view, we predict that the Arctic Ocean basin will not become a large atmospheric CO_2 sink under ice-free conditions.

The CO_2 concentration in the atmosphere has increased greatly since the industrial revolution, and ~30% of the CO_2 released has been taken up by the ocean. This process slows the increase of this greenhouse gas in the atmosphere and thus global warming (*1*), but will likely affect ocean ecosystems via acidification (*2*, *3*). The Arctic Ocean has great potential for taking up atmospheric CO_2 owing to high biological production in the large ocean margin areas and low temperature (*4*, *5*). A recent synthesis suggested that the Arctic Ocean, though constituting only 3% of the world's ocean surface area and mostly ice-covered, accounts for 5 to 14% of the total ocean CO_2 uptake (*6*). This value is highly uncertain, however, owing to relatively few observations and rapid climate changes. The Arctic is widely viewed as the area on Earth most sensitive to climate changes (*1*), with acidification more pronounced than that of any other ocean (*2*). Sea ice melt in the Arctic Ocean has increased steadily over recent decades, proceeding faster in the past three summers (2007 to 2009) than any model prediction (Fig. 1) (*7*–*9*). It has been postulated that an ice-free condition in the Arctic Ocean basins would allow for uptake of a substantial amount of additional CO_2 from the atmosphere (*6*). How CO_2 concentrations in the Arctic surface water may change in response to sea ice melt is, therefore, an important issue for the scientific community and general public.

In the summer of 2008, we conducted a high-resolution underway survey of partial pressure of CO_2 (pCO_2) across the Canada Basin in the western Arctic Ocean where substantial melting of ice had occurred (Fig. 1 and fig. S1). Surface-water temperature was as high as 0° to 5°C in the central Canada Basin (Fig. 2A). Extensive ice melt in this region resulted in salinity values as low as 24 parts per thousand (‰) (Fig. 2B) and ice concentration less than 15% (Fig. 1). Compared to an earlier underway survey in summer 1999, temperatures had increased by 3°C and salinities decreased by ~2‰ (Fig. 2, D and E). During the Arctic Ocean Section (AOS) study in summer 1994, all areas north of 72°N were under ice cover (Fig. 1) with surface seawater temperatures below −1.5°C and salinities above 30‰ (Fig. 2, D and E).

During the summer of 2008, surface-water pCO_2 was below the atmospheric level (~375 μatm) in the entire survey area (Fig. 2C). The lowest pCO_2 (120 to 250 μatm) occurred in marginal sea areas, in agreement with earlier observations (*4*, *10*–*13*). In the ice-free region of the Canada Basin to the northeast, however, there was a large area of relatively high pCO_2 (320 to 365 μatm) that had not been observed before. It contrasted sharply with pCO_2 values of 260 to 300 μatm in the summer of 1999 and the very low pCO_2 (<260 μatm) from the summer of 1994 (Fig. 2F). Further north (≥77°N), where melting of ice in 2008 was less extensive, pCO_2 dropped quickly to below 280 μatm (Fig. 2C). Surface pCO_2 also decreased from the central Canada Basin to areas west of 170°W, where ice cover was relatively heavy, temperature was lower, and salinity was higher.

In ocean margin areas where pCO_2 was very low, dissolved inorganic carbon (DIC) was greatly depleted relative to alkalinity (TA), a quasi-conservative tracer (Fig. 3). Such a DIC decrease indicates net ecosystem production of organic carbon or removal of CO_2 in the surface mixed layer (*5*). In the ice-free region of the Canada Basin, however, both DIC and TA followed the theoretical mixing line of seawater and ice meltwater, indicating no appreciable net biolog-

[1]Department of Marine Sciences, University of Georgia, Athens, GA 30602, USA. [2]Key Lab of Global Change and Marine Atmospheric Chemistry, Third Institute of Oceanography, SOA, Xiamen 361005, China. [3]Korea Polar Research Institute, Incheon 406-840, Republic of Korea. [4]Laboratory of Marine Ecosystem and Biogeochemistry, Second Institute of Oceanography, SOA, Hangzhou 310012, China. [5]Ocean Chemistry Division, National Oceanic and Atmospheric Administration–Atlantic Oceanographic and Meteorological Laboratory, Miami, FL 33149, USA. [6]Cooperative Institute of Marine and Atmospheric Sciences, University of Miami, Miami, FL 33149, USA. [7]Research Institute for Global Change, Japan Agency for Marine-Earth Science and Technology, Yokosuka, Kanagawa 237-0061, Japan. [8]Chesapeake Biological Laboratory, University of Maryland Center for Environmental Science, Solomons, MD 20688, USA. [9]Department of Fisheries and Oceans, Ocean Sciences Division, Bedford Institute of Oceanography, Dartmouth, Nova Scotia, Canada B2Y 4A2.

*To whom correspondence should be addressed. E-mail: wcai@uga.edu